

Supporting Information for

BA₂XBr₄ (X = Pb, Cu, Sn): From Lead to Lead-Free Halide Perovskite Scintillators

Lina Jaya Diguna,^{1, a)} Luke Jonathan,¹ Muhammad Haris Mahyuddin,² Arramel,^{3, 4} Francesco Maddalena,⁵ Irma Mulyani,⁶ Djulia Onggo,⁶ Abdellah Bachiri,⁷ Marcin E. Witkowski,⁷ Michal Makowski,⁷ Dominik Kowal,⁸ Winicjusz Drozdowski,^{7, b)} and Muhammad Danang Birowosuto^{8, c)}

¹⁾ *Department of Renewable Energy Engineering, Universitas Prasetiya Mulya, Kavling Edutown I.1, Jl. BSD Raya Utama, BSD City, Tangerang 15339, Indonesia.*

²⁾ *Research Group of Advanced Functional Materials and Research Center for Nanoscience and Nanotechnology, Institut Teknologi Bandung, Jl. Ganesha 10, Bandung 40132, Indonesia.*

³⁾ *Department of Physics, National University of Singapore, 2 Science Drive 3 Singapore 117551, Singapore.*

⁴⁾ *Nano Center Indonesia, Jl. PUSPIPTEK, South Tangerang, Banten 15314, Indonesia.*

⁵⁾ *CINTRA UMI CNRS/NTU/THALES 3288, Research Techno Plaza, 50 Nanyang Drive, Border X Block, Level 6, Singapore 637553, Singapore.*

⁶⁾ *Inorganic and Physical Chemistry Research Group, Faculty of Mathematics and Natural Sciences, Institut Teknologi Bandung, Jl. Ganesha 10, Bandung 40132, Indonesia.*

⁷⁾ *Institute of Physics, Faculty of Physics, Astronomy, and Informatics, Nicolaus Copernicus University in Torun, ul. Grudziadzka 5, Torun 87-100, Poland.*

⁸⁾ *Lukasiewicz Research Network-PORT Polish Center for Technology Development, Stabłowicka 147, 54-066 Wrocław, Poland*

(Dated: 14 May 2022)

a) Electronic mail: lina.diguna@prasetiyamulya.ac.id

b) Electronic mail: wind@fizyka.umk.pl

c) Electronic mail: muhammad.birowosuto@port.lukasiewicz.gov.pl

Sheet List

Supplementary Figure S1. Rietveld refinement of powder XRD diffractograms of (a) BA_2PbBr_4 , (b) BA_2CuBr_4 , and (c) BA_2SnBr_4 , and (d) Comparison of XRD diffractograms of BA_2CuBr_4 experiment and CuBr_2 in monoclinic phase.

Supplementary Figure S2. (a) Spin-up and (b) spin-down band structure (left panel), corresponding total (black) and projected (color) density of states (right panel) of BA_2CuBr_4 .

Supplementary Figure S3. XPS spectra of (a) C 1s, (b) N 1s, and (c) Br 3d of BA_2XBr_4 (X = Pb, Cu, Sn).

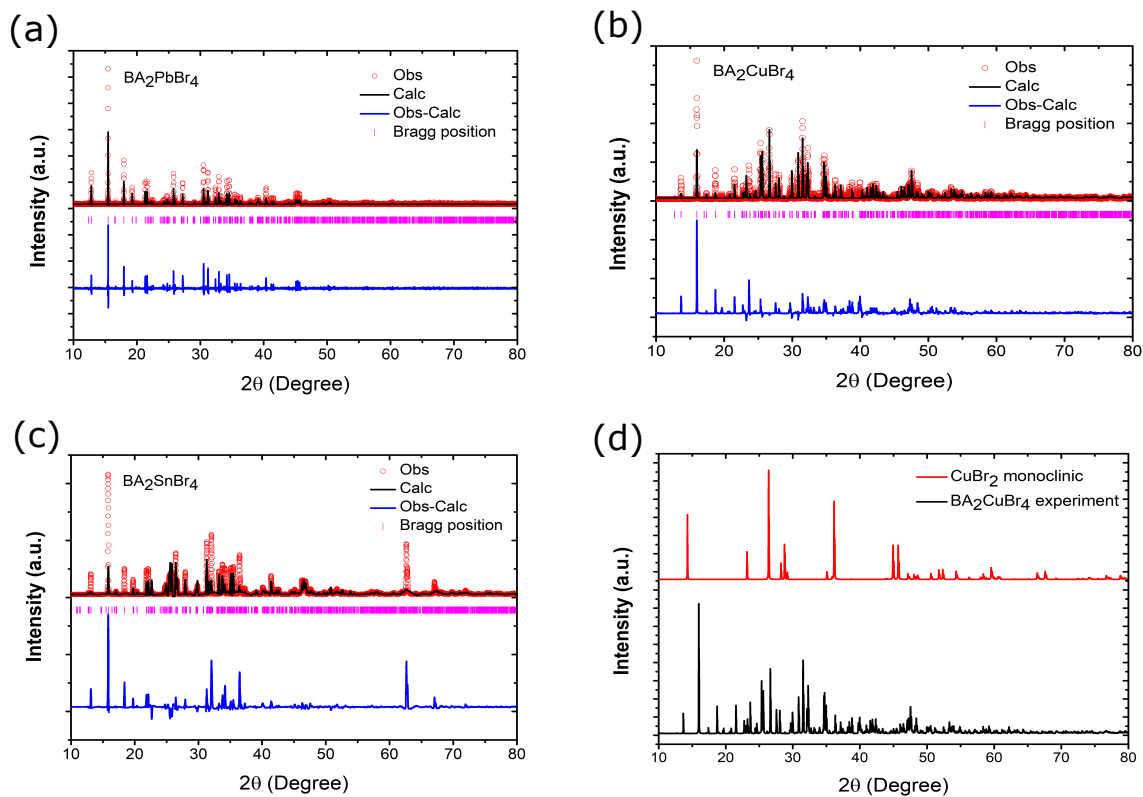
Supplementary Figure S4. Tauc plot of (a) BA_2PbBr_4 , (b) BA_2CuBr_4 , and (c) BA_2SnBr_4 .

Supplementary Figure S5. The fit of glow curve of BA_2SnBr_4 crystals with multiple Randal-Wilkins equation.

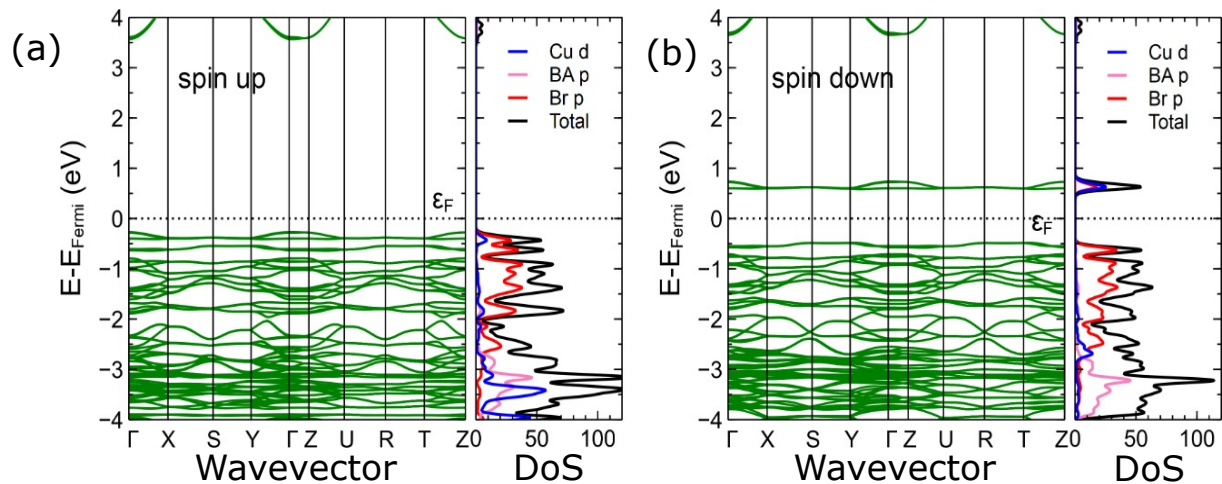
Supplementary Table S1. Fitting parameters for the (negative) thermal quenching of the scintillation intensity of the perovskites.

Supplementary Figure S6. PL spectra recorded with integrating sphere of $(\text{BA})_2\text{XBr}_4$ (X = Pb, Cu, Sn) crystals.

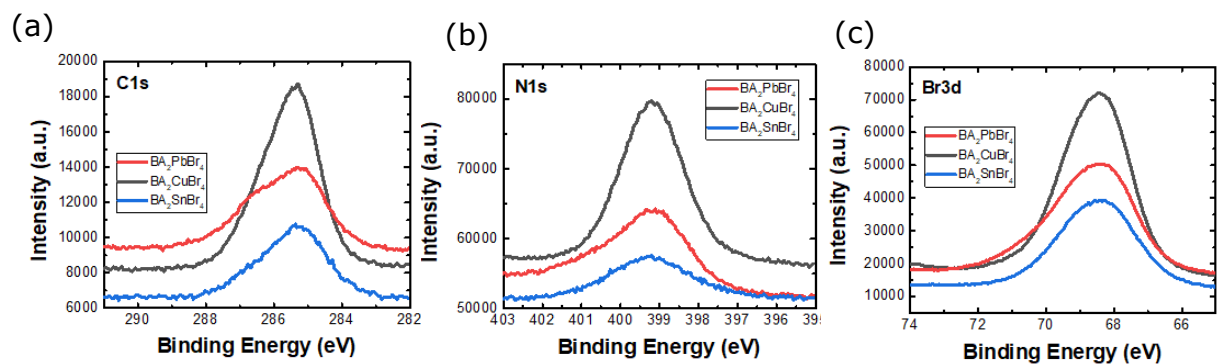
Supplementary Table S2. A summary of the extracted PLQY of the single crystals.



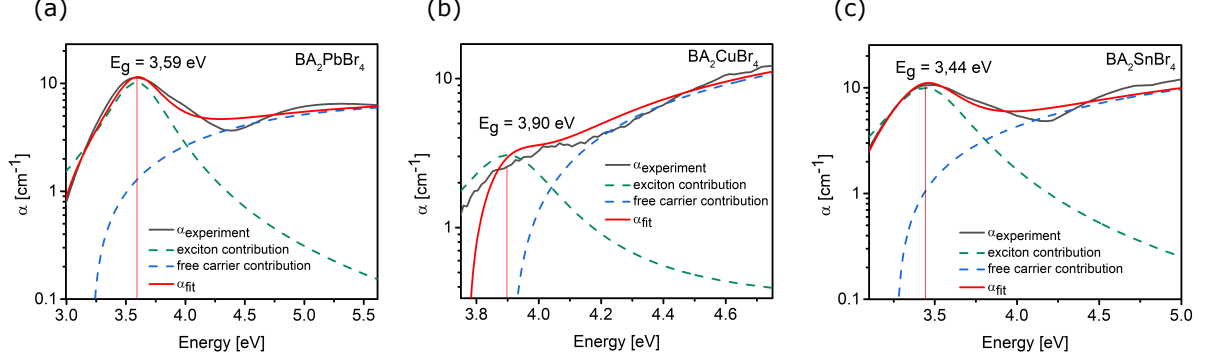
Supplementary Figure S 1: Rietveld refinement of powder XRD diffractograms of (a) BA_2PbBr_4 , (b) BA_2CuBr_4 , and (c) BA_2SnBr_4 , and (d) Comparison of XRD diffractograms of BA_2CuBr_4 experiment and CuBr_2 in monoclinic phase. Reliability factors for BA_2PbBr_4 : $\chi^2 = 4.65$, R-factor = 10.5, $R_p = 91.1$, $R_{wp} = 61.5$. Reliability factors for BA_2CuBr_4 : $\chi^2 = 23.8$, R-factor = 29.0, $R_p = 113.0$, $R_{wp} = 64.4$. Reliability factors for BA_2SnBr_4 : $\chi^2 = 49.9$, R-factor = 22.0, $R_p = 79.7$, $R_{wp} = 68.4$.



Supplementary Figure S 2: (a) Spin-up and (b) spin-down band structure (left panel), corresponding total (black) and projected (color) density of states (right panel) of BA_2CuBr_4 .



Supplementary Figure S 3: XPS spectra of (a) C 1s, (b) N 1s, and (c) Br 3d of BA_2XBr_4 ($\text{X} = \text{Pb}, \text{Cu}, \text{Sn}$).



Supplementary Figure S 4: Absorption spectra from (a) BA_2PbBr_4 , (b) BA_2CuBr_4 , and (c) BA_2SnBr_4 and their fitting curves with Elliot method in Equations S1 and S2.

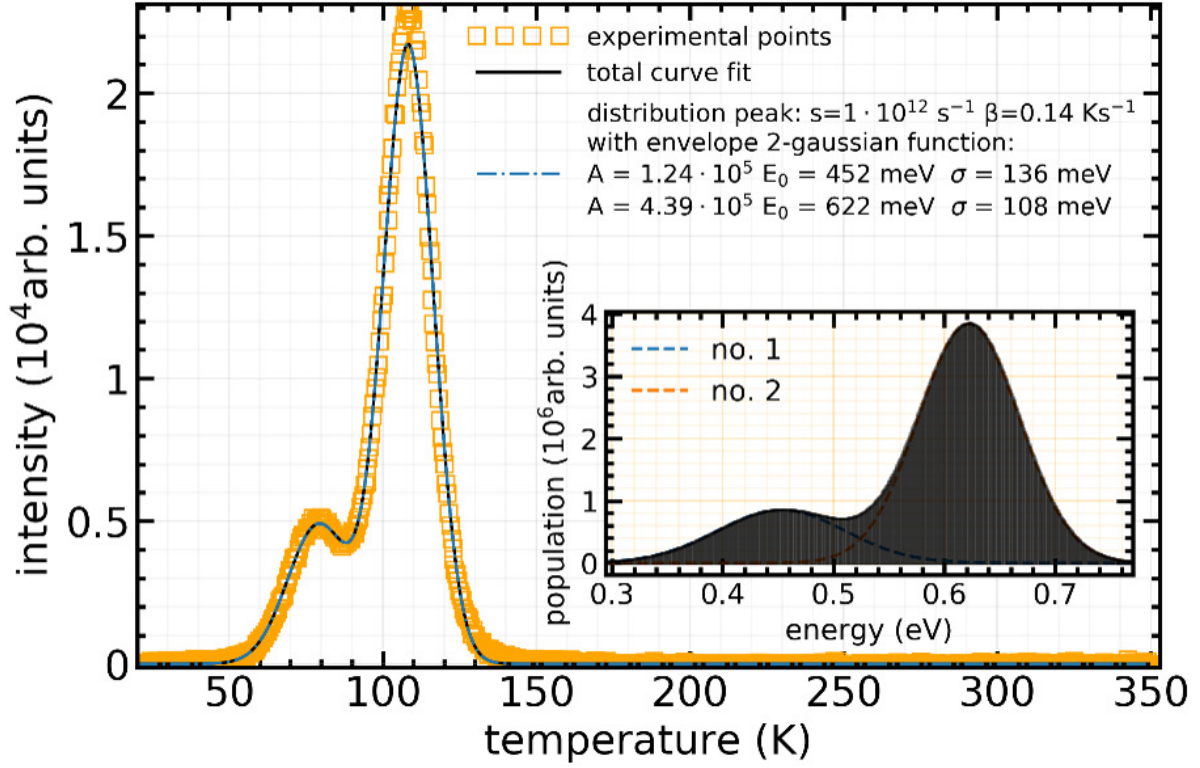
I. FITTING ABSORPTION CURVES

The fit was performed by using Elliot formalism¹. In principle, the contributions to the absorption coefficient (α) can be defined from free carriers (continuum) (α_c) and excitons (α_{ex}).

$$\alpha(\hbar\omega) = \alpha_c + \alpha_{ex} \quad (\text{S1})$$

$$\alpha(\hbar\omega) = P_{cv} \left[\theta(\hbar\omega - E_g) \cdot \left(\frac{\pi e^{\pi x}}{\sinh(\pi x)} \right) + R_{ex} \sum_{n=1}^{\infty} \frac{4\pi}{n^3} \cdot \delta\left(\hbar\omega - E_g + \frac{R_{ex}}{n^2}\right) \right] \quad (\text{S2})$$

Where the frequency dependence of P_{cv} is approximated as a constant and related to the interband transition matrix element, $\hbar\omega$ is the photon energy, $\theta(\hbar\omega - E_g)$ is the Heaviside step function, x is defined as $\sqrt{R_{ex}/(\hbar\omega - E_g)}$, and δ denotes a delta function. R_{ex} is exciton Rydberg energy; n is the principle quantum number. The fits to the absorption curves are shown in Supplementary Figure S4.



Supplementary Figure S 5: The fit of glow curve of BA_2SnBr_4 crystals with multiple Randall-Wilkins equation^{2,3}. The parameters of the fit are shown in the inset.

II. GLOW CURVE FITTING

For the quantitative analysis, we deconvolute the glow curves into k glow peaks, based on the classic Randall-Wilkins equation^{2,3}:

$$I_{TL} = \sum_{i=1}^k n_{0_i} V \sigma_i \exp\left(-\frac{E_i}{k_B T}\right) \exp\left(-\frac{\sigma_i}{\beta} \int_{T_0}^T \exp\left(-\frac{E_i}{k_B T'}\right) dT'\right) \quad (\text{S3})$$

where T is the temperature, β is the heating rate, k_B is the Boltzmann constant, n_{0_i} is the initial trap concentration, V is the crystal volume, E_i is the trap depth, and σ_i is the frequency factor of each component. The unit-less $n_{0_i} V$ or A_i in Supplementary Figure S5 is used to compare afterglow of different crystals.

III. FITTING TEMPERATURE-DEPENDENT RL

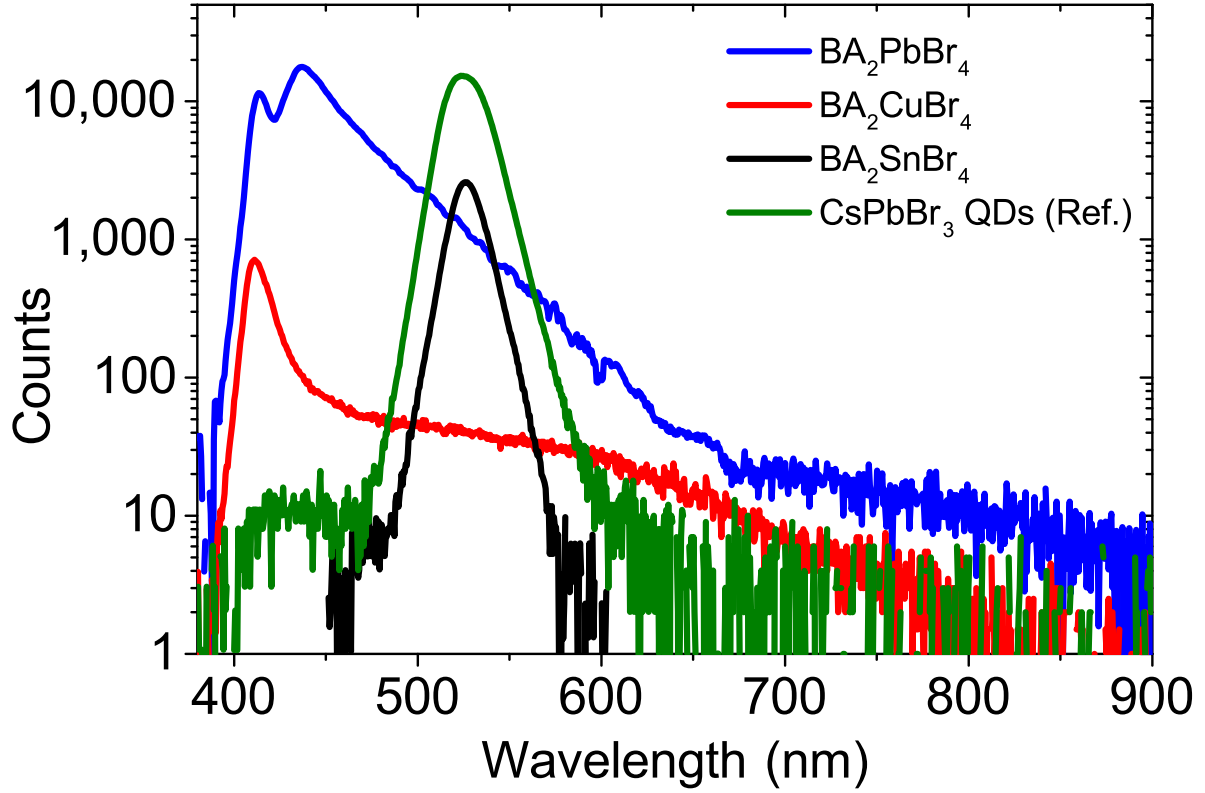
The fit was carried out according to the model proposed by Shibata et al.⁴:

$$\|I(T)\| = \frac{1 + D \cdot e^{-E/k_B T}}{1 + C_1 \cdot e^{-E_1/k_B T} + C_2 \cdot e^{-E_2/k_B T}}$$

where D is the negative thermal quenching coefficient which describes the contribution from thermally excited electrons, C_1 and C_2 are the thermal quenching coefficients related to non-radiative electrons excitation leading to thermal quenching, E is the activation energy for negative thermal quenching and E_1 and E_2 are the activation energies for typical thermal quenching, respectively and k_B is the Boltzmann constant.

Compound	C_1	E_1 (meV)	C_2	E_2 (meV)	D	E (meV)
BA ₂ PbBr ₄	1.03×10^6	4.03	0	0	4.96×10^5	4.07
BA ₂ CuBr ₄	8.75×10^3	23.84	4.50×10^2	0.24	3.56×10^2	0.08
BA ₂ SnBr ₄	1.62×10^4	107.41	5.01	7.23	5.14	16.54

Supplementary Table S 1: Fitting parameters for the (negative) thermal quenching of the scintillation intensity of the perovskites.



Supplementary Figure S 6: PL spectra recorded with integrating sphere of $(\text{BA})_2\text{XBr}_4$ ($\text{X} = \text{Pb}, \text{Cu}, \text{Sn}$) crystals. $(\text{BA})_2\text{PbBr}_4$ (blue), $(\text{BA})_2\text{CuBr}_4$ (red), $(\text{BA})_2\text{SnBr}_4$ (black), and CsPbBr_3 QDs (dark green).

IV. QUANTUM YIELD

To determine the PL quantum yield (PLQY) sample (Q_s), the following equation is used:

$$Q_s = Q_r \left(\frac{A_r}{A} \right) \left(\frac{E_s}{E_r} \right) \left(\frac{n_s}{n_r} \right)^2$$

where Q is the PLQY value, n is the refractive index of the crystals, A is the absorbance of the crystals and E is the integrated PL intensity of the emitted light. The subscript “s” and “r” refer to the reference and unknown emitter, respectively. This method is modified from de Mello et al. as here we used a reference sample that was already known its properties.⁵ As a reference, CsPbBr_3 quantum dots incorporated to the resin from Nanolumi was used without further purification.⁶ Those samples already measured in Nanolumi and the results

were obtained from a private communication.⁷ We note that $Q_r = 64.712\%$, $n_r = 2.3$, $A_r = 0.85$. The PL spectra measured by Labsphere integrating sphere can be found in Supplementary Figure S6 above. Based on the analyses of the refractive index, the integrated PL intensity of the emitted light, and the absorbance of the samples, the PLQY (in %) are determined as shown in Supplementary Table S2 below.

Thin Films	PLQY (%)
BA ₂ PbBr ₄	36
BA ₂ CuBr ₄	1
BA ₂ SnBr ₄	13

Supplementary Table S 2: A summary of the extracted PLQY of the single crystals.

The highest PLQY of 36% is recorded for BA₂PbBr₄ and this value well corresponds with previous observations of 2D Mn doped BA₂PbBr₄ and 0D (C₄H₁₆N₃)PbCl₅·H₂O perovskite halide crystals with PLQY values of 26 and 40%, respectively.^{8,9} Moreover, this value is also reasonable with regard to those reported for (C₆H₅CH₂NH₃)₂Pb·Br₄ (BZA₂PbBr₄) exfoliated crystals with the best and average PLQY values of 79% and 60%, respectively.¹⁰ Other data can be obtained through corresponding authors.

REFERENCES

- ¹R. J. Elliott, Phys. Rev. **108**, 1384 (1957).
- ²M. D. Birowosuto, D. Cortecchia, W. Drozdowski, K. Brylew, W. Lachmanski, A. Bruno, and C. Soci, Sci. Rep. **6**, 37254 (2016).
- ³J. T. Randall and M. H. F. Wilkins, Proc. R. Soc. Lond. A **184**, 365 (1945).
- ⁴H. Shibata, Jpn. J. Appl. Phys. **37**, 550 (1998).
- ⁵J. C. de Mello, H. F. Wittmann, and R. H. Friend, Adv. Mater. **9**, 230 (1997).
- ⁶Nanolumi, “Perovskite color enhancement film for premium displays— nanolumi,” (n.d.).
- ⁷E. Chua, personal communication (2021).

- ⁸T. Sheikh and A. Nag, *J. Phys. Chem. C* **123**, 9420 (2019).
- ⁹A. Yangui, R. Roccanova, Y. Wu, M.-H. Du, and B. Saparov, *J. Phys. Chem. C* **123**, 22470 (2019).
- ¹⁰X. Gong, O. Voznyy, A. Jain, W. Liu, R. Sabatini, Z. Piontkowski, G. Walters, G. Bappi, S. Nokhrin, O. Bushuyev, M. Yuan, R. Comin, D. McCamant, S. O. Kelley, and E. H. Sargent, *Nat. Mater.* **17**, 550–556 (2018).